

Equilibrium properties of 3-arm star-shaped polyions: an entropic sampling Monte Carlo study

I. A. Silanteva¹, A. A. Yurchenko¹, P. N. Vorontsov-Velyaminov¹, A. P. Lyubartsev²

¹St. Petersburg State University, Universitetskaya nab., 7/9, St. Petersburg, 199034, Russia

²Stockholm University, Svante Arrhenius väg 16, Stockholm, 10691, Sweden

i.silanteva@spbu.ru, sila3@yandex.ru

PACS 02.70.-c, 02.70.Uu, 05.10.Ln, 05.70.-a, 05.70.Fh, 07.05.Tp, 36.20.-r, 36.20.Hb, 64.60.-i, 64.70.Nd, 64.70.km, 64.70.pj, 65.40.Ba, 65.80.+n, 81.07.Nb, 82.20.Wt, 82.35.Lr, 87.10.Rt, 87.15.ak, 87.16.aj, 87.53.Wz, 87.55.K

DOI 10.17586/2220-8054-2017-8-1-108-120

The entropic sampling Monte Carlo method within Wang-Landau algorithm is applied to investigate properties of a lattice model of strongly charged flexible 3-arm star-shaped polyelectrolyte. The density of states is calculated, from which the canonical properties of the system in a wide temperature range are obtained by simple integration. The effects of the arm length and the short-range monomer-monomer potential on the thermal and structural properties of star polyions are studied. We calculate such characteristics as mean square radius of gyration and its components, the radius vector of the center of mass, components of the tensor of inertia and parameters characterizing the shape of the polyion. In this work, we focus on how these characteristics are influenced by the change of the reduced temperature which, within the considered model, is a parameter combining the effect of real temperature, linear charge density and solvent dielectric permittivity. The coil-globule transition is observed in most of the considered cases, and for the polyions with the longest length of arms (24), the transition from a liquid globule to a solid-like state is observed. Comparison of polyelectrolyte models with neutral ones is given.

Keywords: star-shaped polymer, polyelectrolytes, lattice model, entropic sampling, Monte Carlo method, phase transition, solvent quality.

Received: 10 January 2017

Revised: 23 January 2017

1. Introduction

Recently, polyelectrolytes having star-like architecture have attracted significant attention being actively investigated by using both experimental [1–4] and theoretical [5–14] methods. These macromolecules are widely used in various fields of nanotechnology, for example as a template for the synthesis of nanoparticles [15] or as emitting devices [16–18]. Charged macromolecules easily interact through electrostatic forces with negatively charged DNA, forming stable complexes for further transporting it into a living cell. They may also be used in another area of biomedicine, particularly in diagnostics and tissue engineering, as antibacterial substances and implant materials [19]. So the investigation of such macromolecules is certainly an important issue.

Star polymers are the simplest among the branched ones. It is known that they are qualitatively different from their linear analogs: the increase of branching leads to an increase in the average concentration of monomers within the macromolecule [20–22]. Therefore, the volume effects for branched polymers are more significant than in the case of linear chains. The properties of stars with a small number of arms are close to those of linear polymers. With an increasing number of arms, the molecule approaches a spherical shape, and its properties become closer to those of nanoparticles. While uncharged models have been sufficiently studied, there is still a lack of understanding in the area of polyelectrolytes. There are at least two specific features of charged polymers in comparison with uncharged ones. First, electrostatic interactions are long-ranged, and secondly, the presence of counterions provides osmotic pressure.

Experiments deal mainly with the polydisperse systems with no clearly defined architecture; from these data, it is difficult to obtain the information on the microscopic state of the macromolecules. Analytical description of star shaped polymers is made difficult by their complex architecture, and is often based on simplifying assumptions; e.g. there exist quasi-planar and nonlocal theories [11] based on the assumption that all the ends of arms are fixed on a certain outer surface. Therefore, in this case, computer simulation methods such as molecular dynamics (MD) or Monte Carlo (MC) appear to be very helpful [5–10].

Investigation of equilibrium conformational properties of polyelectrolytes by standard Monte Carlo or molecular dynamics methods may suffer ergodicity problems due to steric hindrance for a polymer chain to cross another polymer chain. This makes achieving of equilibrium canonical distribution more difficult; evidently for star

polymers the problem becomes more severe with increasing the number of arms. In previous works, we have shown that the entropic sampling Monte Carlo method [23–25], modified for polymer simulations [26,27], provides the possibility to investigate conformational and thermodynamic properties of neutral polymers [26], polyelectrolyte chains [27] and uncharged star-shaped polymers [28,29] in a wide temperature range.

The major aim of our study is to use this advanced sampling method to explore equilibrium properties of the star-branched polyelectrolyte over a wide possible range of temperatures within a simple lattice model [26,27], and obtain insight how the length of arms, the monomer-monomer interactions in the polyion and the concentration of the whole system determine its thermal and structural properties. An additional advantage of the used approach is that it provides a means for obtaining results over a wide range of temperatures, including the area of possible structural transitions in a single computer run. Our independent data could be compared with the existing results of other authors obtained using different approaches [9, 11, 22, 30].

The outline of the paper is as follows: description of the model and of the used method is given in sections 2. Section 3 presents the results of research and discussion for two sets of data: a polyion with various length of arms and a polyion with various short-range monomer-monomer interactions. The conclusions are presented in the last, fourth, section.

2. Model and Method

Though lattice models were introduced some time ago, they still have not lost their relevance [31–35]. On the one hand, simple models allow us to run simulations quickly and efficiently, on the other hand absence of chemical details gives possibility to get insight into underlying physical background of the studied phenomena. In this study the model of flexible star shaped polyion on a simple cubic lattice with the lattice constant $a = 1$ is considered. This model was originally proposed in paper [36] and later used in work [27] to study the equilibrium behavior of a polyelectrolyte chain. In our case, the star shaped polyion (for convenience, we shall call it simply a “star”) is located in a cubic cell of the size d with periodic boundary conditions imposed. The regular star consists of f arms, each of which includes N_{arm} monomers; here, we limit ourselves by the cases of $f = 3$. The monomers are located at the lattice sites and are connected to each other in a proper way by rigid bonds of a unit length. The total number of monomers per polyion is $N = fN_{\text{arm}} + 1$, i. e. the arms’ monomers plus the central monomer connecting all the arms and fixed in the center of the periodic cell. We limit ourselves to cases when each monomer carries unchangeable (quenched) unit charge; although, if necessary, the simulation of a partially ionized molecule is also possible. In order to maintain electroneutrality in the cell, N ions (counterions), carrying unit charges of the opposite sign are also present and they can move freely within the cell. The counterions are located on sites of the lattice shifted by the vector $(0.5, 0.5, 0.5)$ relative to the lattice of the polyion location. This excludes overlaps of counterions with the polyion and hence makes the MC procedure more efficient. It should also be noted that the minimal distance of a counterion and a monomer is $\sqrt{3}/2 = 0.866$ while the minimal distance for monomer-monomer and counterion-counterion is 1.

The volume interactions are taken into account while modeling of the polyelectrolyte by forbidding any two monomer units, or any two ions to occupy the same lattice site. However, during the simulation, we allow the star’s monomers to overlap with each other (phantom random walks [37]), as well as overlaps of the mobile counterions, in order to improve sampling. This way, the system achieves compact conformations with extremely low probabilities but still contributing to the canonical averages at low temperatures, due to low energy of these conformations. The overlapping conformations are then excluded from the canonical averaging to obtain the correct statistics for the conformations without overlaps (intersections), according to the procedure described below.

Monomers of the polyion and counterions interact through Coulomb potential $U(r_{ij}) = q_i q_j / r_{ij}$, where q_i and q_j are charges and r_{ij} the distances between them. Thus, the energy of the entire system consists of three components: repulsion between the monomers of the polyion, repulsion between the counterions and attraction between monomers and counterions. All distances are measured in the lattice constant units a , the energy is expressed in units of $E_0 = e^2 / (\epsilon a)$, the temperature is in units of $e^2 / (\epsilon a k_B)$ where e is the elementary charge, ϵ is the dielectric constant of the solution, k_B is Boltzmann constant. So for the temperature in our units we have:

$$T = k_B T_K / E_0, \quad (1)$$

where T_K is temperature in Kelvins.

Let us determine the typical temperature range for aqueous solutions of a real polyelectrolyte system. If the lattice constant is taken equal to the distance between charged groups on the polyelectrolyte chain (for example, 2.8 Å for polyacrylic acid), dielectric constant for water is $\epsilon = 80$, the temperature $T_K = 293$ K would yield $T = 0.39$. Actually, ϵ of water decreases with temperature so that product ϵT_K shows a weak decrease with temperature also, that is why the increase of real temperature T_K in aqueous solution leads to some decrease of

the reduced temperature T . The dielectric permittivity can be also changed by addition of other organic solvents, and the polyelectrolyte linear charge density can be changed by pH of the solution. To summarize, the reduced temperature T of our model is a parameter expressing the collective effect of the polyion charge density, real temperature and properties of the solvent, with typical values 0.3–0.7 for strong polyelectrolytes and with higher values for weaker polyelectrolytes.

In order to present a complete picture of behavior for our model system we are going to obtain dependencies over a much broader temperature range so that we can see how our data are tending to athermal limits. Though not all the temperature range in which the results would be obtained and presented further is achievable in a real laboratory experiment. In order to take into account the long-range electrostatic interactions in presence of periodic boundary conditions the minimal image convention was used in calculating them. It was shown in [27] that it gives for our model the same result as the Ewald summation [38] over a wide range of parameters.

The quality of the solvent, defined by the parameter $\chi = \tilde{z}\Delta w_{12}/k_B T$, [39], where \tilde{z} is the number of nearest neighbors in the model, Δw_{12} is the change of energy in the formation of a contact polymer-solvent in the solution, such interaction also is straightforwardly included into our model (See part 3.2). It is modeled by assigning the energy u_0 to pairs of unbound monomers occupying neighboring lattice sites, $u_0 = -\Delta w_{12}$. The zero value of u_0 corresponds to conditions of a good solvent (See part 3.1). The smaller the parameter u_0 , values correspond to lower solvent qualities χ (χ also depends on the temperature).

The method that we used here is the entropic sampling (ES) method [23, 24] within Wang-Landau (WL) algorithm [25] initially applied to polymers in our simulation group [26] and successfully used later by us [27–29, 34, 37, 40, 41] and by other researchs [30, 33, 42–45] for studying different polymer systems. In the ES-WL computer experiment the density of states $g(E)$ is calculated just as it was done in [27] (see [27] for details). The density of states obtained by this procedure allows us to calculate the canonical averages of physical characteristics over a wide temperature range with the aid of simple summation:

$$\langle F \rangle (T) = \frac{\sum_{i=0}^M F_i g_i e^{-E_i/T}}{\sum_{i=0}^M g_i e^{-E_i/T}}, \quad (2)$$

where F_i is the calculated average of the corresponding physical quantity at conditions corresponding to the i -th energy interval, which is also determined within the simulation. The summation is over the whole energy range (divided into M intervals) that corresponds to conformations of the system without intersections. As the quantity F it can be taken: the configuration energy, the square of the radius of gyration and its components, the modulus of the radius vector of the center of mass, the components of the tensor of inertia. It is worth noting here that at $T \rightarrow \infty$ equation (2) gives the results for the athermal case taking into account the excluded volume interactions of the monomers (a non-charged polymer in a good solvent).

The heat capacity is calculated by the following relationship:

$$C(T) = \frac{\partial E}{\partial T} = \frac{\langle E^2 \rangle (T) - (\langle E \rangle (T))^2}{T^2}. \quad (3)$$

In order to ensure the correct work of the program, we have run it first for linear chains (star with two arms) with the number of monomers $N = 11, 31, 51, 81$ in the same way as it has been done in the previous paper [27]. The size of the cell was chosen so that the concentration c was constant, $d = 30, 42, 50, 58$ respectively. In this case the chain is attached by the center monomer at the center of the periodic cell, and cannot move freely as in [27]. In the presence of periodic boundary conditions, this distinction should not affect the final result. The obtained test data are consistent with the data of work [27], which means that the program can be used for subsequent calculations.

Next, we investigated how the concentration of the solution affected the properties of the studied system with its other parameters being kept constant. We consider the stars with three arms of the length $N_{\text{arm}} = 10$ and change the concentration by the corresponding variation of the periodic cell size d in the range (16, 50) which corresponds to concentrations $c \in [7.57 \cdot 10^{-3}, 2.48 \cdot 10^{-4}]$ respectively (see [46]). Thus, it is possible to confirm the assertion that increasing the concentration of the solution results in a decrease in the swelling of the polyelectrolyte star [22]. The change of concentration in the studied range does not lead to qualitative changes in the thermal and structural properties of the investigated system.

3. Results

3.1. The effect of the length of arms

In order to study how the properties of 3-arm polyelectrolyte star depend on the length of arms we consider the samples with the following length of arms: $N_{\text{arm}} = 10, 15, 19, 24$; respectively the total number of monomers is $N = 31, 46, 58, 73$. The size of the cell was selected so that the polymer concentration remains approximately the same for all the considered cases and its value is $c \approx 4.2 \cdot 10^{-4}$. The corresponding sizes of the cells are $d = 42, 48, 52, 56$. Short-range monomer-monomer interactions are not included.

Figure 1 shows the logarithm of the density of states function for conformations of stars with various N_{arm} . One can see that with an increase in the length of arms the maximum of the distribution shifts to higher energies, and the range of possible energies expands. The lowest energy corresponds to the conformation of a dense globule with built-in counterions; at increasing energy, the counterions leave the star polyion which is transferred to a swollen state; at a positive energy the star loses the counterions completely. At highly-positive energies, very compact conformations without counterions are observed, which do not contribute significantly to the canonical averaging.

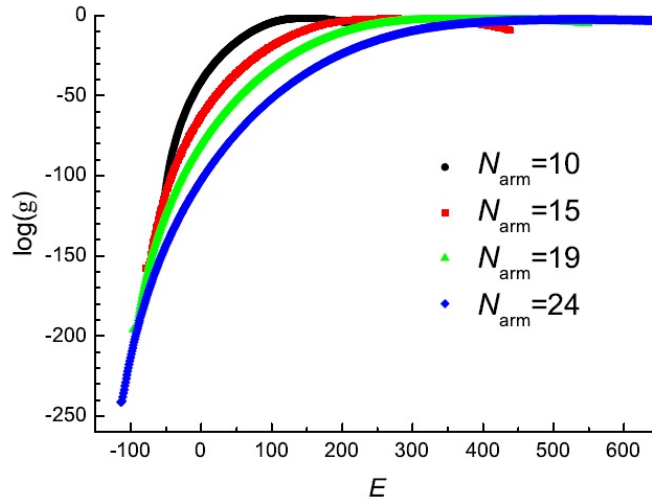


FIG. 1. The logarithm of the density of states as a function of energy for conformations of the 3-arm stars with different lengths of arms $N_{\text{arm}} = 10, 15, 19, 24$

Average configuration energy of stars (Fig. 2a) increases monotonously with increasing temperature. The same way as in the case of chains [27], there exists a point at which the graphs intersect, i.e. it is the temperature at which the energy does not depend on the number of monomers in the star. A similar behavior was observed for uncharged stars [41] with a contact negative interaction potential between monomers. It should especially be noted here that while for ordinary electrolyte solutions the equilibrium configurational energy is always negative with the limiting value being zero for $T \rightarrow \infty$, in the case of polyelectrolyte containing a polyion with rigid bonds the energy can become positive with an increase in temperature. This is because polymer bonds cannot dissociate and the energy of polyion-polyion interaction remains positive while polyion-ion and ion-ion interaction energies tend to zero, the case that we observe in our data.

Each dependency (Fig. 2b) has a broad non-smooth maximum for the heat capacity, which indicates a coil-globule transition. With an increase in the arm length, an additional maximum is observed at low temperatures, and in the case of the star with $N_{\text{arm}} = 24$ a sharp peak emerges. Similar peaks for long chain polyelectrolytes ($N > 50$) were observed by Volkov et. al. [27]. An analogous result was obtained in [30], where the bond-fluctuation lattice model for the uncharged star polymer was studied; the authors attributed this peak to a liquid \rightarrow crystal-like state transition. Also, with an increase of the N_{arm} , some small rippling on the curves appears, that could be apparently associated with the specific features of the lattice model or with discrete splitting of the energy range into intervals, and, we believe, they do not carry much physical sense.

Let us watch now the structural properties starting with the square of the radius of gyration:

$$R_g^2 = \frac{1}{2N^2} \sum_{i=1}^N \sum_{j=1}^N |r_{ij}|^2 = \frac{1}{N} \sum_{i=1}^N (r_i - \vec{R}_c)^2, \quad (4)$$

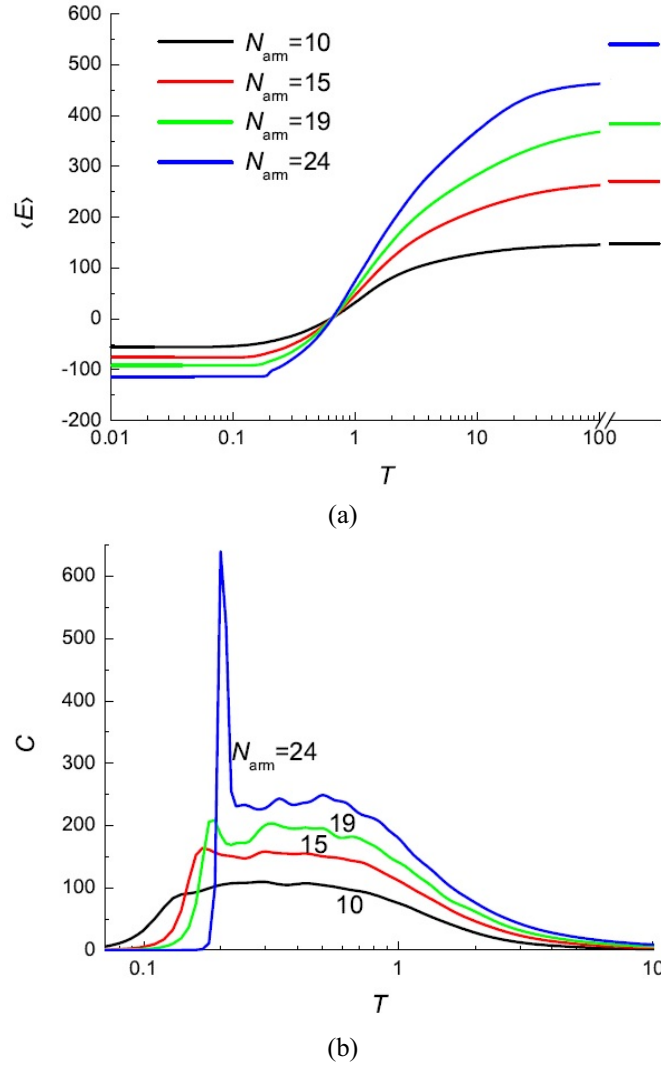
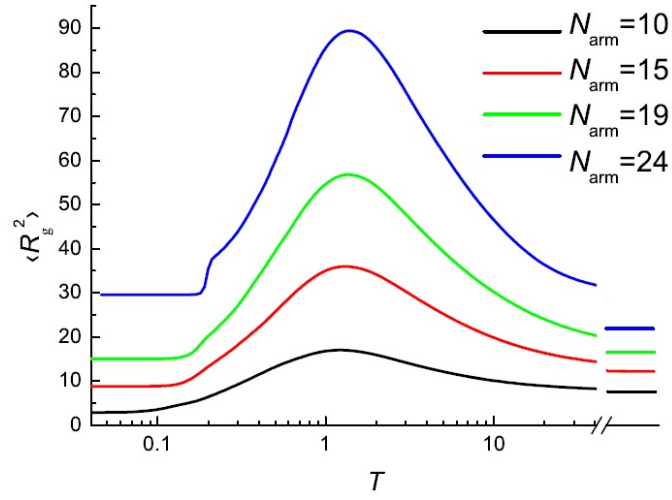


FIG. 2. The temperature dependence of the average configuration energy (a) and of heat capacity (b) for the stars ($f = 3$) with different lengths $N_{\text{arm}} = 10, 15, 19, 24$. The horizontal dashes on the right of this and the next graphics show the values at $T \rightarrow \infty$, i. e. the values for athermal case

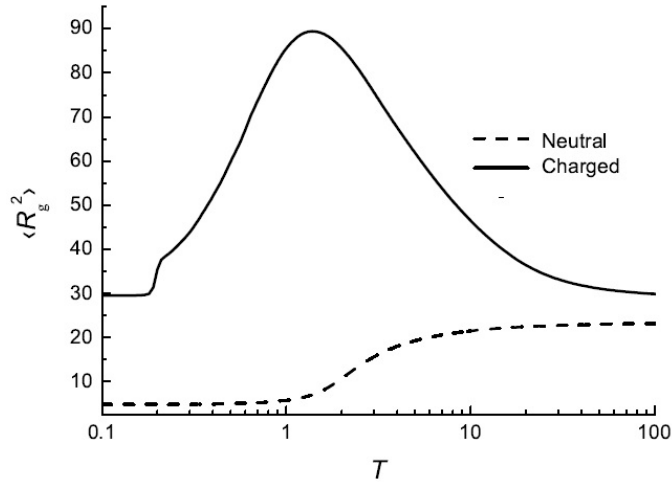
where \vec{R}_c is the radius vector of the center of mass. The temperature dependence of $\langle R_g^2 \rangle(T)$ has the following form (Fig. 3a): a single maximum in the vicinity of $T \approx 1.2$ (varies for different N_{arm}). Its value increases with increasing N_{arm} , and its position is slightly shifted to higher temperatures. In this range the polymer is in a swollen state, its size is several times larger than the size of the ideal polymer. It is worth noting here that for the uncharged model of a star (with a negative interaction potential) [28, 29] the dependence of $\langle R_g^2 \rangle(T)$ has a simple monotonic rise (Fig. 3b). So the maximum observed in the case of polyelectrolyte is caused by the presence of electrostatic interactions. At low temperatures ($T < 0.1$) the star polyion is in a compact state with built-in counterions, and its size is determined only by the total number of segments.

At high temperatures, when $k_B T$ is considerably higher than the energy of electrostatic interaction the effect of the latter is insignificant. This is the area of so-called athermal solvent in terms of Flory theory (Flory-Huggins parameter $\chi = 0$) [39]. The values of athermal limits ($T \rightarrow \infty$) for $\langle R_g^2 \rangle(T)$ dependence (dashes in Fig. 3a) can be approximated as $\langle R_g^2 \rangle(T) \propto N^{1.21}$, that coincides with scaling predictions from analytical theories [12, 20] for an uncharged star in a good solvent.

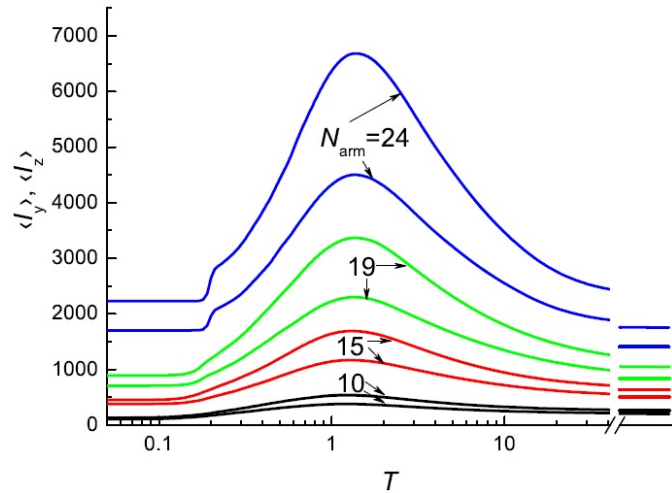
All the components of the inertia tensor were also obtained at each step and its matrix was reduced to a diagonal form to extract three main components. The averaged reduced components of the inertia tensor $\langle I_x \rangle < \langle I_y \rangle < \langle I_z \rangle$ are shown in Fig. 3c. It is evident that in the entire considered temperature range the components have different



(a)



(b)



(c)

FIG. 3. Temperature dependencies of the average values of: the mean square radius of gyration $\langle R_g^2 \rangle$ (a), the reduced components $\langle I_y \rangle, \langle I_z \rangle$ of the tensor of inertia, $\langle I_y \rangle < \langle I_z \rangle$ ($\langle I_x \rangle$ not shown for clarity, the form of dependence is similar to $\langle I_y \rangle, \langle I_z \rangle$) (c) for the stars ($f = 3$) with different length of arms $N_{\text{arm}} = 10, 15, 19, 24$. Comparison of $\langle R_g^2 \rangle(T)$ for charged and neutral stars, $f = 3, N_{\text{arm}} = 24$ (b)

values and by rotational properties each star can be described as a three-axial ellipsoid elongated along one axis (cucumber).

In order to characterize the shape in more detail, the components of the mean square radius of gyration were also calculated (Stockmayer [47, 48]) L_1^2, L_2^2, L_3^2 , so that $R_g^2 = L_1^2 + L_2^2 + L_3^2$, $L_1^2 < L_2^2 < L_3^2$. Firstly all the components of the tensor were calculated:

$$L_{lk}^2 = \frac{1}{N} \sum_{i=1}^N (r_{il} - R_{cl})(r_{ik} - R_{ck}), \quad l, k = 1, 2, 3, \quad (5)$$

where R_{cl} and R_{ck} are the l -th and k -th coordinates of the center of mass vector. Then the matrix of the tensor was reduced to a diagonal form and three components were determined. Knowledge of the three components provides possibility to determine the parameter that allows us to distinguish the oblate shape from the elongated one (Fig. 4a):

$$S^* = (3sf_1 - 1)(3sf_2 - 1)(3sf_3 - 1). \quad (6)$$

Here, the reduced components emerge $sf_1 = L_1^2/R_g^2$, $sf_2 = L_2^2/R_g^2$, $sf_3 = L_3^2/R_g^2$. Parameter S^* varies in the range $[-0.25, 2]$, and can be both negative (oblate shape) and positive (prolate shape) [32]. At $T \approx 1.2$ the star is in a swollen state, its shape is close to spherical ($S^* \approx 0$, Fig. 4a), and its conformation is asymmetric relative

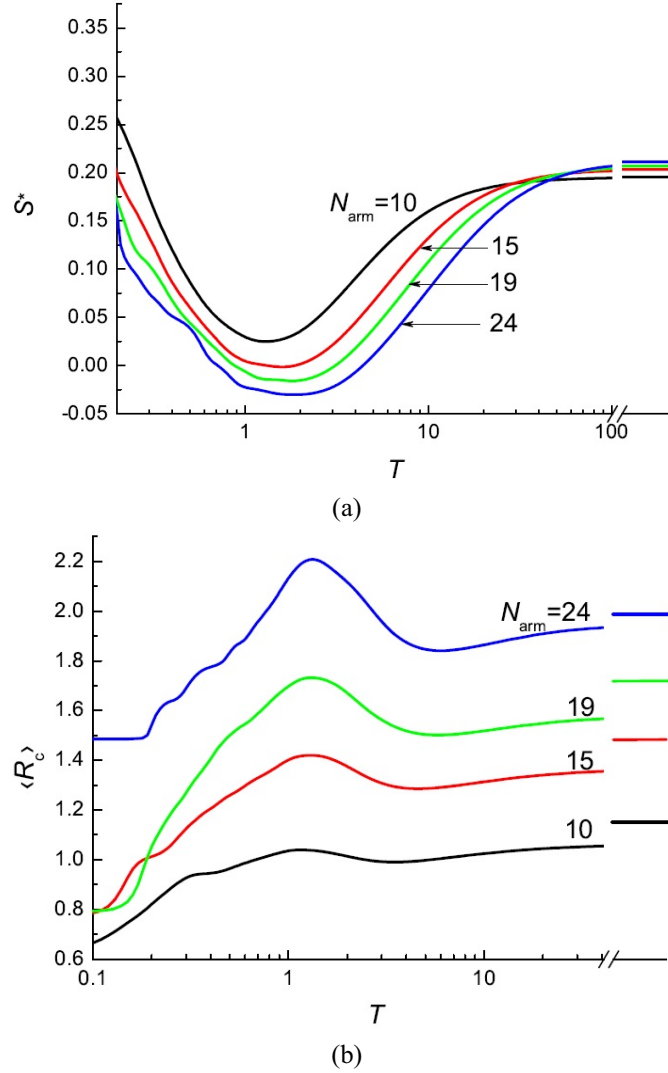


FIG. 4. Temperature dependencies of the parameter characterizing the shape S^* (a), of the average modulus of the radius vector of the center of mass $\langle R_c \rangle$ (b) for 3-arm stars with different length of arms $N_{\text{arm}} = 10, 15, 19, 24$

to its center (maximum $\langle R_c \rangle (T)$ Fig. 4b). At $T \rightarrow 0$ the size of the star decreases, the conformation becomes symmetric relative to the center (decreasing $\langle R_c \rangle (T)$).

The analytical theory for the salt-free dilute solution of star-shaped electrolyte was proposed in [22]. It gives the scaling relations that allow us to estimate the size of the stars R for separate regimes. The first is the unscreened regime, which is achieved if $Q \ll R/l_B$, where Q is the total charge of the star, $l_B = e^2/\epsilon k_B T$ is the Bjerrum length. In this case the star size is determined by the following relationship [22]:

$$R \cong N_{\text{arm}} m^{-2/3} l_B^{1/3} f^{1/3}, \quad (7)$$

where $1/m$ is the part of ionized monomers. In our case, the polymer is completely ionized, and $m = 1$. In this regime counterions surround the star and there is a dependence of the star size on the number of arms.

The second regime is osmotic, which is achieved when $Q \gg R/l_B$. In this case the star captures and holds the counterions from the solution. Its size does not depend on the number of arms and is determined by the relation:

$$R \cong N_{\text{arm}} m^{-1/2}. \quad (8)$$

If we consider the results of this theory in the framework of our model, we obtain the following. In the units of our model $l_B = 1/T$, and the first regime is reached when $RT \gg Q$, i. e. at high temperatures, and $R \cong N_{\text{arm}} T^{-1/3} 3^{1/3}$. This regime corresponds to the decreasing dependence of $\langle R_g^2 \rangle (T)$ (Fig. 3a). The osmotic regime is achieved when $RT \ll Q$ is provided.

We can qualitatively compare our results with work [9], where the classical MC simulation is carried out for star-branched micelles with $N_{\text{arm}} = 130$ and with the number of arms 6 and 27 in some range of temperatures. There, the dependence of R_g/N_{arm} on the parameter ζ is presented; ζ corresponds to $1/T$ in the units of our model. $R_g/N_{\text{arm}}(\zeta)$ dependence is not monotonic and has a maximum in the area around $\zeta = 1$ similar to our case (see $\langle R_g^2 \rangle (T)$ and its maximum in Fig. 3a). Each $\langle R_g^2 \rangle (T)$ dependence has a single broad maximum in the vicinity of $T \approx 1.2$, the height of the maximum is determined by the length of arms in a star. The unscreened regime is observed at $T \gg 1$ ($\zeta \ll 1$). With a decrease in temperature, when the Coulomb energy of counterions in the field, created by the corona radius [9] becomes of the order of $k_B T$, the regime of spherical condensation is achieved. It is performed at $\zeta_{\text{sph}} \approx 1/f$, i.e. $T_{\text{sph}} \approx f$. When all counterions are inside the star, the osmotic regime is observed [22], in [9] it occurs at $\zeta \gg 1/f$. In our case the number of arms is small and osmotic regime is observed around the maximum of $\langle R_g^2 \rangle (T)$, it becomes broader with increasing f . We analyzed $\langle R_g^2 \rangle$ values (Fig. 3a) in the area of $1 < T < 1.38$, and obtained that $\langle R_g^2 \rangle (T) \propto N_{\text{arm}}^2$, which agrees with eq. (8).

When the Manning criterion of cylindrical condensation [49] is satisfied, i.e. $\zeta > 1$ or $T < 1$ the counterion condensation around each arm of the star begins. In this regime, the condensed counterions partly compensate the charge of the star polyion, and the effective charge fraction of the star becomes $\alpha_{\text{eff}} = T$. So the size of the star at the same time is decreased, see Fig. 3a. With further decreasing of temperature the transition of polyion into the collapsed state that was predicted by Schissel and Pincus [50] for strongly charged chains is observed. We can see this state at $T < 0.1$, Fig. 3a. When the collapse energy dominates over the entropic contribution, each counterion is attached to a monomer and forms an electric dipole [9, 50, 51]. The attraction of the dipoles leads to a transition to a collapsed state. It can be noted here that in [9], the collapsed state is not achieved probably due to the consideration of a limited temperature range.

Thus, we can conclude that for star and linear polyions within the above considered model at the increasing the number of monomers there appears a transition from a liquid to a solid-like state in addition to the coil-globule transition. It is shown how strongly the polyelectrolyte star swells compared to the uncharged polymer.

3.2. The effect of the short-range interactions

In this series of simulations, we investigate how the short-range (contact) interactions influence the star polyion properties. We consider a 3-arm star with $N_{\text{arm}} = 10$ in the cell of size $d = 42$, that corresponds the concentration $c \approx 4.2 \cdot 10^{-4}$. The contact attraction of unbound monomers, located at a distance of the lattice constant are determined by the energy $u_0 < 0$, that is varied in the range $[-3; 0]$. Note that the smaller is the parameter u_0 is, the worse is the quality of the solvent χ .

The logarithm of the density of states as a function of energy is presented in Fig. 5. One can see that with decreasing of the parameter u_0 values, the range of possible energies significantly expands to the negative E -side, which is to be expected. Maximum of $g(E)$ shifts to the lower energies and the coordinates of maxima at the E -axis are 154.56, 145.55, 144.06, 141.93, 136.10, 131.09 for $u_0 = 0, -0.2, -0.5, -1, -2, -3$ respectively. It is not simply a left shift of $g(E)$ function for the case of $u_0 = 0$, the shape of the $g(E)$ changes with u_0 as well.

The temperature dependences of the average configuration energy $\langle E \rangle$, and of excess free energy ΔF are presented in Fig. 6a. One can see that the curves are qualitatively close to each other for different u_0 values and

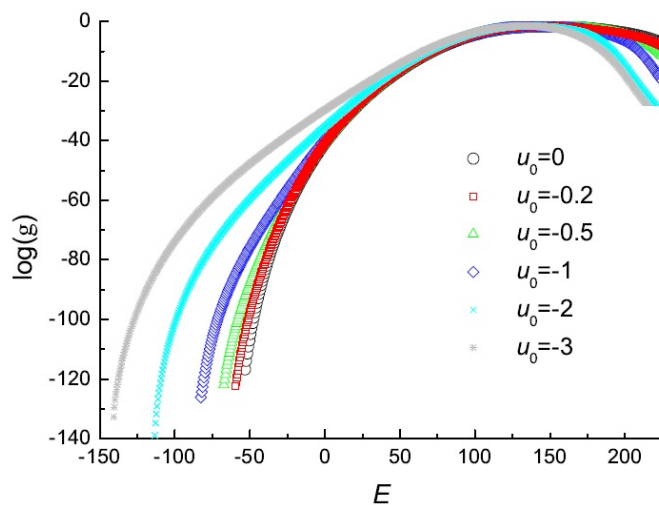


FIG. 5. The logarithm of the density of states as a function of energy for conformations of the 3-arm star ($N_{\text{arm}} = 10$) at different u_0 parameter values, $u_0 = 0, -0.2, -0.5, -1, -2, -3$

only the energy of the ground state becomes lower for lower u_0 . At $T \rightarrow 0$ the values of $\langle E \rangle$ and ΔF for each case tend to the common limits.

The maximum of $C(T)$ dependence (Fig. 6b) becomes sharper and noticeably shifts to the right at T axis with lowering of the parameter u_0 . One can see that the addition of the short-range attractive potential results in easier transition to the globule state, and this transition becomes not as smooth as in the case of $u_0 = 0$. The $\langle R_g^2 \rangle(T)$ dependence is presented in Fig. 7a; we can notice that the addition of the short-range attractive potential results in decreasing of the polyelectrolyte swelling. The coil-globule transition now occurs at higher temperatures. The maximum of $\langle R_g^2 \rangle(T)$ is shifted to the higher temperature region. At low T the values of $\langle R_g^2 \rangle(T)$ for $u_0 \neq 0$ tends to the common limit that is slightly lower than for the case of $u_0 = 0$. This slight difference could be caused by insufficient statistics for the low-energy conformations that was discarded at averaging. We suppose that the size of the globule must be independent of u_0 .

We consider the shape of the star using the asphericity parameter:

$$\delta = 1 - 3(sf_1sf_2 + sf_2sf_3 + sf_3sf_1). \quad (9)$$

Here, the reduced components are the same as in the equation (6). The asphericity parameter varies from zero (absolute symmetry, sphere) to one (form of a rigid rod).

$\delta(T)$ and $S^*(T)$ dependencies are presented in Fig. 7b,c. Before the transition to the globule state the shape of the star polyion becomes elongated that we can conclude from observing the maxima of $\delta(T)$ and $S^*(T)$. These maxima become significantly sharper with decreasing u_0 values.

It was shown how the addition of the short-range attraction potential affects the size and shape of a 3-arm star polyion. It was confirmed that the short-range attraction potential results in easier transition from a coil to a globule state. The greater the attraction, the stronger the asymmetric shape of the molecule is before transition into a globular state.

4. Conclusion

In this work, the entropic sampling Monte Carlo method is applied to study the lattice model of the 3-arm star-shaped polyelectrolyte with constant (quenched) charges and with short-range attractive interaction of the monomers in a salt-free solution. The applied approach allows us to trace the equilibrium state of the considered system over a wide temperature range, including athermal, unscreened, osmotic, Mannings condensation and collapsed regimes.

Two sets of calculations were performed. In the first set, the length of arms was modified at fixed overall density of the system. For comparatively short arms the temperature decrease results in the transition of the coil-globule type while with increasing the arm lengths there appears an additional transition from a liquid-like to a solid-like state. We can see that for the polyelectrolyte the $\langle R_g^2 \rangle(T)$ dependency has a maximum while it rises monotonously for the neutral ones, the swelling of the polyelectrolyte is much larger than that for neutral stars.

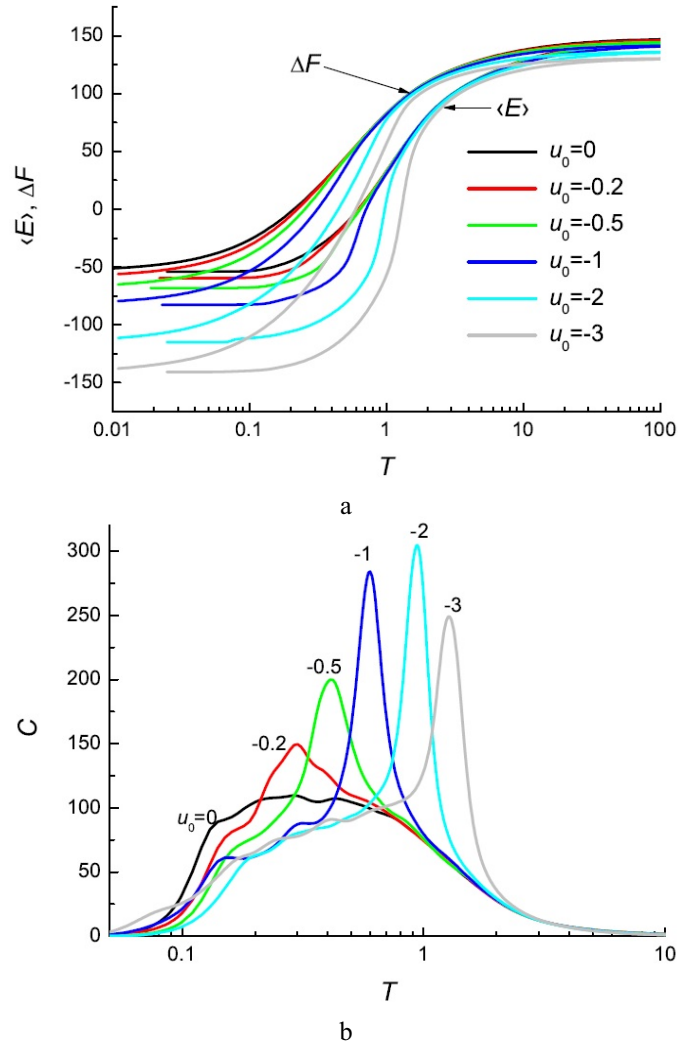


FIG. 6. The temperature dependence of the average configuration energy $\langle E \rangle$, of excess free energy ΔF (a) and of heat capacity C (b) of the 3-arm star ($N_{\text{arm}} = 10$) at different values of the parameter u_0 , $u_0 = 0, -0.2, -0.5, -1, -2, -3$

In the second set of simulations, the short-range monomer-monomer interactions that characterize the solvent quality are included. It is shown that short-range monomer-monomer attraction results in an easier transition from a coil to a globule state and with a more elongated molecule shape before transition into a globular state.

In this work, we have studied systems with comparatively small number of monomers $N < 73$ that can be considered as a starting point for further work. It can include increasing the number of arms, their length, as well as considering the system with the addition of salt ions of different valence. It should be pointed out here that the studied case without added salt is perhaps more difficult for simulations because the salt ions create additional screening of electrostatic interactions, and at high concentrations, the properties of charged macromolecules approach the properties of the neutral ones [13,22]. Change of the charge fraction on the polyion (which models change of solvent pH) can also be envisioned.

Considering continuous models and combining the method applied here with other approaches (MD, expanded ensemble MC, etc.) could be used as well. The algorithm can be straightforwardly parallelized with the use of multiwalker sampling which would allow us to use the method for substantially larger systems. Particularly, it would permit increasing the length of star arms and their number. This way, further study would seemingly yield new interesting results in the area of branched polyelectrolytes.

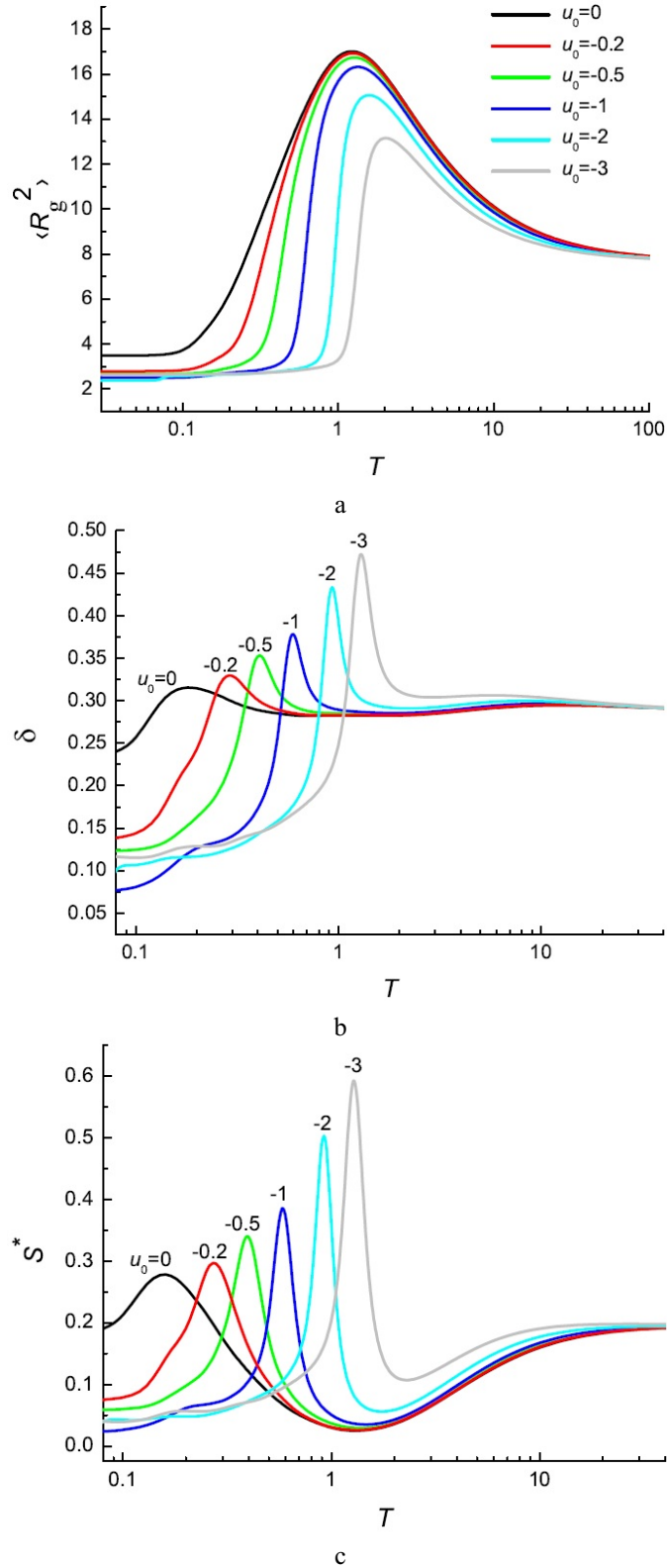


FIG. 7. Temperature dependencies of the averaged square radius of gyration $\langle R_g^2 \rangle$ (a), of the asphericity parameter δ (b), of the parameter characterizing the shape S^* (c) of the 3-arm star ($N_{\text{arm}} = 10$) at different u_0 parameter values, $u_0 = 0, -0.2, -0.5, -1, -2, -3$

Acknowledgements

This work is supported by the St. Petersburg State University, the project numbers 11.37.290.2015, 11.57.673.2014, 11.57.159.2016.

References

- [1] Alhoranta A. M., Lehtinen J. K., Urtti A. O., Butcher S. J., Aseyev V. O., Tenhu H. J. Cationic amphiphilic star and linear block copolymers: synthesis, self-assembly, and in vitro gene transfection. *Biomacromolecules*, 2011, **12**, P. 3213–3222.
- [2] Aryal S., Prabaharan M., Pilla S., Gong S. Biodegradable and biocompatible multi-arm star amphiphilic block copolymer as a carrier for hydrophobic drug delivery. *International Journal of Biomacromolecules*, 2009, **44**, P. 346.
- [3] Cameron D., Shaver M. Aliphatic polyester polymer stars: synthesis, properties and applications in biomedicine and nanotechnology. *Chemical Society Reviews*, 2011, **40**, P. 1761–1776.
- [4] Filippov A. P., Romanova O. A., Vinogradova L. V. Molecular and hydrodynamic characteristics of star-shaped polystyrenes with one or two fullerene (C₆₀) molecules as a branching center. *Polymer Science A*, 2010, **52** (3), P. 221–227.
- [5] Jusufi A., Likos C. N., Löwen H. Counterion-induced entropic interactions in solutions of strongly stretched, osmotic polyelectrolyte stars. *J. Chem. Phys.*, 2002, **116**, P. 11011.
- [6] Jusufi A., Likos C. N., Löwen H. Conformations and Interactions of Star-Branched Polyelectrolytes. *Phys. Rev. Lett.*, 2001, **88**, P. 018301.
- [7] Jusufi A., Likos C. N. Colloquium: Star-branched polyelectrolytes: The physics of their conformations and interactions. *Rev. Mod. Phys.*, 2009, **81**, P. 1753–1772.
- [8] Likos C. N., Blaak R., Wynveen A. Computer simulations of polyelectrolyte stars and brushes. *J. Phys.: Condens. Matter*, 2008, **20**, P. 494221.
- [9] Roger M., Guenoun P., Muller F., Belloni L., Delsanti M. Monte-Carlo simulations of star-branched polyelectrolyte micelles. *Eur. Phys. J. E.*, 2002, **9**, P. 313–326.
- [10] Košovan P., Kuldová J., Limpouchová Z., Procházka K., Zhulina E. B., Borisov O. V. Molecular dynamics simulations of a polyelectrolyte star in poor solvent. *Soft Matter*, 2010, **6**, P. 1872–1874.
- [11] Zhulina E. B., Birshtein T. M., Borisov O. V. Curved polymer and polyelectrolyte brushes beyond the Daoud-Cotton model. *Eur. Phys. J. E.*, 2006, **20**(3), P. 243–256.
- [12] Birshtein T. M., Mercurieva A. A., Leermakers F. A. M., Rud O. V. Conformations of polymer and polyelectrolyte stars. *Polymer Science A*, 2008, **50**(9), P. 992–1007.
- [13] Polotsky A. A., Zhulina E. B., Birshtein T. M. Effect of the ionic strength on collapse transition in star-like polyelectrolytes. *Macromol. Symp.*, 2009, **278**, P. 24–31.
- [14] Rud O. V., Mercurieva A. A., Leermakers F. A. M., Birshtein T. M. Collapse of Polyelectrolyte Star. Theory and Modeling. *Macromolecules*, 2012, **45**(4), P. 2145–2160.
- [15] Kytseval N. V., Rawiso M. Star-shaped dextran-polyacrylamide polymers. Features of the structure and prospects of application in nanotechnology. *Vestnik Kazanskogo Technologicheskogo Universiteta*, 2014, **17**(2), P. 164–169 (in Russian).
- [16] Montgomery N., Hedley G., Ruseckas A., Denis J., Schumacher S., Kanibolotsky A., Skabara P., Galbraith I., Turnbull G., Samuel I. Dynamics of fluorescence depolarisation in star-shaped oligofluorene-truxene molecules. *Phys. Chem. Chem. Phys.*, 2012, **14**, P. 9176–9184.
- [17] Swinarev A., Piekarnik B., Grobelny Z., Stolarzewicz A., Simokaitiene J., Andrikaityte E., Grazulevicius J. Star-Shaped Poly((9-carbazolyl)methylthiirane): A New Polymer for Optoelectronic Applications. *Macromol. Symp.*, 2011, **308**(1), P. 8–11.
- [18] Zang Z.-L., Zou L.-Y., Ren A.-M., Liu Y.-F., Feng J.-K., Sun C.-C. Theoretical studies on the electronic structures and optical properties of star-shaped triazatruxene/heterofluorene co-polymers. *Dyes and Pigments*, 2013, **96**(2), P. 349–363.
- [19] Wu W., Wang W., Li J. Star polymers: Advances in biomedical applications. *Progress in Polymer Science*, 2015, **46**, P. 55–85.
- [20] Likos C. N. Soft matter with soft particles. *Soft Matter*, 2006, **2**, P. 478–498.
- [21] Muzafarov A. M., Vasilenko N. G., Tatarinova E. A., Ignateva G. M., Myakushev V. M., Obrezkova M. A., Meshkov I. B., Voronina N. V., Novozhilov O. V. Macromolecular nano-objects as a promising direction of polymer chemistry. *Polymer Science C*, 2011, **53**(1) P. 48.
- [22] Klein Wolternik J., Leermakers F. A. M., Fleer G. J., Koopal L. K., Zhulina E. B., Borisov O. V. Screening in solutions of star-branched polyelectrolytes. *Macromolecules*, 1999, **32**, P. 2365–2377.
- [23] Berg B. A., Neuhaus T. Multicanonical ensemble: a new approach to simulate first-order phase transitions. *Phys. Rev. Lett.*, 1992, **68**, P. 9–12.
- [24] Lee J. New Monte Carlo algorithm: entropic sampling. *Phys. Rev. Lett.*, 1993, **71**, P. 211–214.
- [25] Wang F., Landau D. P. Efficient, multiple-range random walk algorithm to calculate the density of states. *Phys. Rev. Lett.*, 2001, **86**, P. 2050–2035.
- [26] Vorontsov-Velyaminov P. N., Volkov N. A., Yurchenko A. A. Entropic sampling of simple polymer models within Wang-Landau algorithm. *J. Phys. A*, 2004, **37**, P. 1573–1588.
- [27] Volkov N. A., Vorontsov-Velyaminov P. N., Lyubartsev A. P. Entropic sampling of flexible polyelectrolytes within the Wang-Landau algorithm. *Phys. Rev. E*, 2007, **75**, P. 016705.
- [28] Silantyeva I. A., Vorontsov-Velyaminov P. N. The calculation of the density of states and the thermal properties of the polymer chains and stars on a lattice by Monte Carlo method using the Wang-Landau algorithm. *Numerical Methods and Programming*, 2011, **12**, P. 397–408 (in Russian).
- [29] Silantyeva I. A., Vorontsov-Velyaminov P. N. Thermodynamic properties of star shaped polymers investigated with Wang-Landau Monte Carlo simulations. *Macromol. Symp.*, 2012, **317–318**, P. 267–275.
- [30] Wang Z., He X. Phase transition of a single star polymer: a Wang-Landau sampling study. *J. Chem. Phys.*, 2011, **135**, P. 094902.
- [31] Clisby N. Efficient implementation of the pivot algorithm for self-avoiding walks. *J. Stat. Phys.*, 2010, **140**, P. 349–392.
- [32] Zifferer G., Eggerstorfer D. Monte Carlo simulation studies of the size and shape of linear and star-branched copolymers embedded in a tetrahedral lattice. *Macromol. Theory. Simul.*, 2010, **19**, P. 458–482.

- [33] Wüst T., Lee Yu., Landau D. Unraveling the beautiful complexity of simple lattice model polymers and proteins using Wang-Landau sampling. *J. Stat. Phys.*, 2011, **144**, P. 638–651.
- [34] Yurchenko A. A., Antyukhova M. A., Vorontsov-Velyaminov P. N. Investigation of the interaction of the polymer with the surface by entropic modeling. *J. Structure Chemistry*, 2011, **52**(6), P. 1216–1223 (in Russian).
- [35] Vogel T., Bachmann M., and Janke W. Freezing and collapse of flexible polymers on regular lattices in three dimensions. *Phys. Rev. E*, 2007, **76**, P. 061803.
- [36] Lyubartsev A. P., Vorontsov-Velyaminov P. N. Monte-Carlo modeling of flexible polyelectrolytes. *Polymer Science U.S.S.R.*, 1990, **32**, P. 660–666.
- [37] Volkov N. A., Yurchenko A. A., Lyubartsev A. P., Vorontsov-Velyaminov P. N. Entropic sampling of free and ring polymer chains. *Macromol. Theory Simul.*, 2005, **14**, P. 491–504.
- [38] Frenkel D., Smit B. *Understanding molecular simulation: from algorithms to applications*. Academic Press, 2001.
- [39] Grossberg A. Yu., Khokhlov A. R. *Statistical physics of macromolecules*. AIP Press, Woodbury, 1994.
- [40] Silantyeva I. A., Vorontsov-Velyaminov P. N. Entropic sampling of star-shaped polymers with different number of arms: temperature dependencies of structural properties. *Nanosystems: physics, chemistry, mathematics*, 2015, **6**(4), P. 513–523.
- [41] Vorontsov-Velyaminov P. N., Yurchenko A. A., Antyukhova M. A., Silantyeva I. A., Antipina A. Yu. Entropic sampling of polymers: A chain near a wall, polyelectrolytes, star-shaped polymers. *Polymer Science C*, 2013, **55**(1), P. 112–124.
- [42] Janke W., Paul W. Thermodynamics and structure of macromolecules from flat-histogram Monte Carlo simulations. *Soft Matter*, 2016, **12**, P. 642–657.
- [43] Seaton D. T., Wüst T., Landau D. P. Collapse transition in a flexible homopolymer chain: application of the Wang-Landau algorithm. *Phys. Rev. E*. 2010. **81**. 011802.
- [44] Martemyanova J. A., Stukan M. R., Ivanov V. A., Müller M., Paul W., Binder K. Dense orientationally ordered states of a single semiflexible macromolecule: An expanded ensemble Monte Carlo simulation, *J. Chem. Phys.*, 2005, **122**, P. 174907.
- [45] Wang Z., Wang L., Chen Y., He X. Phase transition behaviours of a single dendritic polymer. *Soft Matter*, 2014, **10**, P. 4142–4150.
- [46] Silanteva I. A., Vorontsov-Velyaminov P. N. Entropic sampling study of star-shaped polyelectrolytes on a lattice. Proceedings of “Multiscale modeling of materials and molecules”, Uppsala, Sweden, 7–9 June 2016. P. 6.
- [47] Šolk K., Stockmayer W. H. Shape of a RandomFlight Chain. *J. Chem. Phys.*, 1971, **54**(6), P. 2756–2757.
- [48] Šolk K. Shape of a RandomFlight Chain. *J. Chem. Phys.*, 1971, **55**, P. 335–344.
- [49] Manning G. S. Limiting Laws and Counterion Condensation in Polyelectrolyte Solutions I. Colligative Properties. *J. Chem. Phys.*, 1969, **51**, P. 924–933.
- [50] Schiessel H., Pincus P. Counterion-Condensation-Induced Collapse of Highly Charged Polyelectrolytes. *Macromolecules*, 1998, **31**(22), P. 7953–7959.
- [51] Brilliantov N., Kuznetsov D., Klein R. Chain Collapse and Counterion Condensation in Dilute Polyelectrolyte Solutions. *Phys. Rev. Lett.*, 1998, **81**(7), P. 1433.